Simulating translation-induced laser speckle dynamics in photon Doppler velocimetry

Will J. Warren,* Erik A. Moro, Matthew E. Briggs, and Eric B. Flynn

Los Alamos National Laboratory, P.O. Box 1663, Los Alamos, New Mexico 87545, USA

*Corresponding author: wwarren@lanl.gov

Received 10 April 2014; revised 28 May 2014; accepted 13 June 2014;
posted 13 June 2014 (Doc. ID 209914); published 14 July 2014

Historically, single-beam optical velocimetry has been limited to measuring only the component of velocity along the beam. However, theoretical work and recent experimental results have shown that laser speckle dynamics may be exploited to measure lateral motion, thereby gaining information about surface dynamics across an additional degree of freedom. In the use of photon Doppler velocimetry (PDV), this new information is considered "free" in that it is already contained within the PDV signal, needing only to be extracted and interpreted correctly. In this manuscript, we relate speckle dynamics to the lateral motion of a planar scattering surface in the PDV coordinate system via the space–time correlation function of the diffracted electric field. Next, we relate the characteristic time scale of speckle intensity fluctuations in the PDV signal to the rate of lateral surface translation and to parameters characterizing the optical probe. Analytical results are compared with a numerical simulation and found to be in close agreement.

OCIS codes: (030.6140) Speckle; (120.7250) Velocimetry; (060.2370) Fiber optics sensors.
http://dx.doi.org/10.1364/AO.53.004661

1. Introduction

Photon Doppler velocimetry (PDV) is an optical diagnostic that has recently become popular in shock physics studies due to its accuracy [1,2], high bandwidth, and ease of fielding. The heterodyne technique measures velocity along a laser beam's path. Surface motion along the beam imparts a Doppler-shift on backscattered light that, when combined with a reference field, produces a beat frequency from which axial velocity may be resolved.

Random speckle is produced from the scattering of coherent light off of an optically rough surface; conditions that are characteristic of PDV experiments, which employ 1550 nm light. The resulting de-phased wave fronts extend outward from the surface, combining to form an interference pattern manifested by regions (or elongated lobes [3]) of varying light intensity across three-dimensional space. Speckles are measured in the PDV signal as low frequency intensity fluctuations that modulate the amplitude of the desired heterodyne signal. While typically seen as an undesirable, yet unavoidable consequence of coherent light interference, theoretical work and recent experimental results have shown that the characteristic time scale of these speckle intensity fluctuations is related to lateral surface speed.

A surface's speckle pattern is a random but fixed property of that surface, reproducible if illuminated in a consistent manner. As the surface gradually moves through the illumination, the spatial structure of the resulting speckle pattern gradually changes with time. This variation in the speckle pattern's spatial structure is referred to as speckle dynamics. According to our current understanding, speckle dynamics can be broadly defined by two behaviors: translation and boiling. Translation refers to the coherent bulk motion of speckle in a given geometry, which, in our case, is related to the lateral motion of the scattering surface. Boiling refers to the

1559-128X/14/214661-08$15.00/0

incoherent behavior of speckles randomly fading in and out of existence, erratically shifting through space without favoring any specific geometry. Speckle intensity fluctuations measured in the PDV signal may be explained by speckle dynamics, which, in turn, may be explained by surface motion.

While the spatial structure of speckle is manifested by complex, random patterns of varying light intensity, the statistical properties of speckle are orderly and quantifiable [4,5]. In the same way, speckle dynamics are governed by statistical properties that reliably describe variation in a speckle pattern's spatial structure due to lateral surface motion. A large body of theoretical and experimental work has explored the dynamic behavior of speckle for a transmission geometry in which a focusing optic directs a laser beam *through* a transparent laterally translating diffuser onto a detector that lies beyond. Rather than attempt to review existing works, the reader is referred to Yoshimura [6], who consolidates the mathematical concepts of speckle dynamics for the transmission geometry established by Takai and co-workers [7–11]. In PDV applications, light is reflected from the scattering surface rather than transmitted through it. Since the PDV probe both focuses the laser beam onto the reflective surface and acts as a detector by collecting backscattered light, the PDV geometry has one degree of freedom rather than two.

Under the strict assumptions of pure speckle pattern translation, and a point-like detector located in the far-field of a transparent laterally translating diffuser, Iwai *et al.* [12] show that the characteristic time scale of speckle intensity fluctuations is given by

$$\tau_c = \frac{\omega_0}{|v_\perp|}, \tag{1}$$

where ω_0 is the radius of the illuminating laser beam at the focal point and $v_\perp$ is the surface velocity vector, perpendicular to the laser beam's optical path. Recent experimental work [13] applied this model to PDV to simultaneously measure axial velocity and lateral surface speed with a single probe. Despite differences in geometry and requisite assumptions, lateral speed estimates were distributed within roughly 30% of the ground truth for the tested optical conditions. Subsequent work [14,15] found that τ_c changes depending upon the location of the translating surface along the laser beam.

Since PDV is inherently used to gather data from surfaces moving along the laser beam and through its focal length, speckle dynamics must be understood, along with how their parametric dependencies influence lateral speed measurement capabilities. Furthermore, to make use of speckle dynamics in PDV applications, one must consider a surface whose velocity vector contains both lateral and axial velocity components. This paper attempts to set up the full three-dimensional problem by first evaluating speckle dynamics in the PDV coordinate system for a surface whose motion is perpendicular to the laser beam's optical path. To the best of the authors' knowledge, this is the first paper to analytically examine speckle dynamics for the PDV coordinate system, which is different from the transmission geometry that has received so much attention in the past.

In this manuscript, we examine the relationship between speckle dynamics and lateral surface motion for the PDV coordinate system, both analytically and through a simulation approach. Simulation allows us to directly investigate the underlying physics that are expressed in our analytical equations and to avoid experimental uncertainties.

2. Theoretical Model

The PDV coordinate system is shown in Fig. 1. An optical probe, centered in the observation plane (x,y), directs a laser beam onto the parallel scattering surface (α,β), offset by axial displacement z. Light is then scattered back onto the observation plane where a speckle pattern is observed. Data are measured from the portion of backscattered light that transmits back into the probe aperture.

For this particular free-space geometry, speckle formation is modeled by the Fresnel diffraction integral, which expresses the value of a complex field at arbitrary point (x,y,z) as the summation of many random elementary phasors. Using a Huygens approximation, each phasor may be thought of as a spherical wavefront extending outward from the scattering surface with some unique magnitude and phase. The superposition of these wavefronts at (x,y,z) produces interference, a random walk in the complex plane, and a single resultant amplitude. The complex field produced at the observation plane $\mathbf{A}(x,y,z,t)$ is directly related to the complex field incident on the scattering surface $\mathbf{a}(\alpha,\beta,z,t)$ through

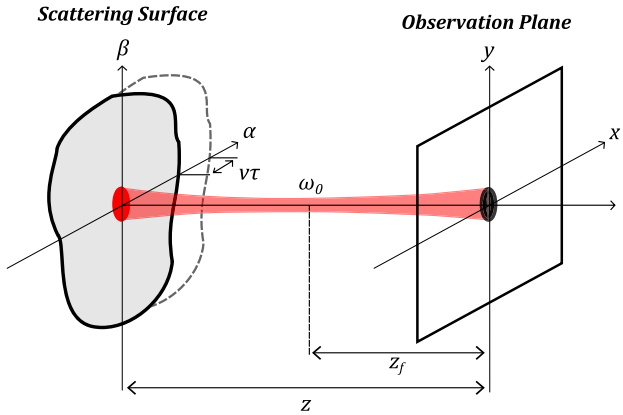

Fig. 1. PDV optical arrangement and coordinate system. A Gaussian laser beam is directed onto the scattering surface (α,β); a measured signal is produced from the portion of scattered light that returns back through the probe aperture (black circle), centered at the origin of the observation plane (x,y). The beam focal point is located at a fixed distance z_f from the observation plane.

the point spread function of free-space, mathematically expressed

$$\mathbf{A}(x,y,z,t) = \frac{e^{ikz}}{i\lambda z} e^{\frac{ik}{2z}(x^2+y^2)} \times \int^{\infty} \int_{-\infty} \mathbf{a}(\alpha,\beta,z,t) e^{\frac{ik}{2z}(\alpha^2+\beta^2)} e^{-\frac{ik}{z}(x\alpha+y\beta)} \mathrm{d}\alpha \mathrm{d}\beta, \tag{2}$$

where λ is the wavelength of light and $k = 2\pi/\lambda$. By considering spatial frequencies $(f_x, f_y) = (x/\lambda z, y/\lambda z)$, note that Eq. (2) may be regarded as a Fourier-transformation [16].

Scattered field $\mathbf{a}(\alpha,\beta,z,t)$ is the product of an illumination function, which describes the distribution of light incident over the scattering surface, and a phase variation term that arises from the implicit roughness of the scattering surface. In PDV experiments, a Gaussian beam is used for illumination and the scattering surface is typically a diffuse metal. We assume the scattering surface translates in-plane in the positive α-direction at arbitrary constant speed v. Under these conditions, $\mathbf{a}(\alpha,\beta,z,t)$ is given by

$$\mathbf{a}(\alpha,\beta,z,t) = \underbrace{\frac{\omega_0}{\omega} \exp\left[-(\alpha^2+\beta^2)\left(\frac{1}{\omega^2} + \frac{ik}{2\rho}\right) - ikz\right]}_{\text{Gaussian beam illumination}} \underbrace{\times \exp[i\phi(\alpha+vt,\beta)]}_{\text{surface-induced phase variation}}. \tag{3}$$

The shape of a Gaussian beam is completely defined by the focal length (z_f) and beam waist (ω_0) of its focusing optic. Since the beam originates at the optical probe centered in the observation plane, the size of the illuminated beam spot over the scattering surface depends upon the axial displacement z between the scattering surface and observation plane, shown in Fig. 1. The radius of the illuminated beam spot over the scattering surface, defined as the radial distance from the origin where the intensity falls to e^{-2} times the maximum intensity, is expressed

$$\omega = \omega_0 \left(1 + \frac{(z-z_f)^2}{a^2}\right)^{1/2} \tag{4}$$

with $a = \pi\omega_0^2/\lambda$. The Gaussian illumination function is complex-valued and the form of its phase component over the scattering surface is determined by the beam radius of curvature at the point of incidence, given

$$\rho = (z-z_f)\left(1 + \frac{a^2}{(z-z_f)^2}\right). \tag{5}$$

Light scattering is complicated, involving shadowing, masking, volume scattering, and specular reflection components. We adopt a simplified model in which light propagating to the surface changes phase as a function of surface-height and the wavelength of light, according to

$$\phi(\alpha,\beta) = \frac{2\pi}{\lambda} h(\alpha,\beta), \tag{6}$$

for zero mean surface-height function $h(\alpha,\beta)$. We use a common idealization of a rough surface called the deep random-phase screen: a white noise process for which $\phi(\alpha,\beta)$ is a random distribution that is uniform over the primary interval $[-\pi,\pi]$, and which ensures the formation of a fully developed speckle pattern.

In application, one must employ a detecting element of finite size to receive backscattered light; for PDV applications, this detecting element is the aperture of the optical probe. It follows that the PDV signal is produced by integrating the diffracted intensity field $\mathbf{I}(x,y,z,t)$ over a finite region of the observation plane, given by

$$\mathbf{W}(z,t) = \int^{\infty} \int_{-\infty} \mathbf{D}(x,y)\mathbf{I}(x,y,z,t)\mathrm{d}x\mathrm{d}y, \tag{7}$$

for aperture function $\mathbf{D}(x,y)$. The intensity of the backscattered field is given $\mathbf{I} = \mathbf{A}\mathbf{A}^*$, where $(^*)$ denotes the complex conjugate. For a circular probe of radius R centered in the observation plane, the aperture function is defined

$$\mathbf{D}(x,y) = \begin{cases} 1 & \text{if } \sqrt{x^2+y^2} \le R \\ 0 & \text{otherwise} \end{cases}. \tag{8}$$

We assume that our photodetector is ideal, in that a signal is produced from light collected over an infinitesimal period of time. Our assumption is justified if the photodetector integration time is much smaller than the time scale of speckle intensity fluctuations in the measured signal, which holds strongly for PDV applications.

3. Simulation

A. Static Speckle

We begin by describing the methods used to simulate a speckle pattern for the static case, when the scattering surface is not in motion. This is accomplished by specifying z, z_f, ω_0, and λ for the Gaussian beam illumination function and generating a random-phase screen $\phi(\alpha,\beta)$ from white noise that is uniformly distributed over the primary interval $[-\pi,\pi]$. Each constituent function is discretized into a 4000 × 4000 matrix where, depending on the propagation distance to the observation plane, individual discretized areas measure between 1 and 4 μm on a side. The element-wise product of these functions constitutes the scattered field, given in Eq. (3). After factoring in the quadratic phase terms from Eq. (2), which are inherent to Fresnel diffraction, the scattered field is propagated out to the observation plane at offset distance z via a Fourier-transform [17, p. 370].

Two optical probes are implemented in the simulation to investigate the parametric dependencies of speckle dynamics on the shape of the laser beam. Both focusing and collimating probes are tested and their parameters given in Table 1. Wavelength λ is set to 1550 nm, which is typical for PDV. Figure 2 provides a visual representation of the constituent functions and speckle pattern that is produced in the simulation for Probe 1 at $z = 40$ mm.

B. Speckle Dynamics

Speckle dynamics describe variation in a speckle pattern's spatial structure with respect to time. For lateral surface motion, speckle dynamics are characterized by translation and boiling. While we are ultimately interested in predicting lateral surface motion from speckle intensity fluctuations measured in the PDV signal, it is useful to understand the general relationships between scattering surface motion and speckle dynamics. Our motivation in this section is twofold: to gain an intuitive understanding for the behavior of dynamic speckles and to verify that our simulation reproduces this behavior. To this end, we will focus on answering two primary questions:

- If the scattering surface is translating in a given orientation, does the resulting speckle pattern translate in the same orientation and at the same rate?
- How far must the scattering surface translate before the resulting speckle pattern decorrelates, effectively becoming unrecognizable?

We quantify the above questions analytically and numerically by evaluating the space–time cross-correlation function of the diffracted electric field, effectively measuring the similarity between intensity field $\mathbf{I}_1$ produced at time t, and intensity field $\mathbf{I}_2$ produced at arbitrary time $(t+\tau)$, expressed

$$\langle \mathbf{I}_1 \mathbf{I}_2 \rangle = \langle \mathbf{I}(x,y,z,t)\mathbf{I}(x+\Delta x, y+\Delta y, z, t+\tau)\rangle, \quad (9)$$

where $\langle \ldots \rangle$ indicates an ensemble average. We normalize the correlation function to the range [0,1], where 1 indicates that two speckle patterns are identical and a value below e^{-1} indicates that the two speckle patterns are effectively uncorrelated. The normalized correlation function [6] is given by

$$\boldsymbol{\mu}_I(\Delta x, \Delta y, z, \tau) = \frac{\langle \mathbf{I}_1 \mathbf{I}_2 \rangle}{\langle \mathbf{I}_1 \rangle \langle \mathbf{I}_2 \rangle} = 1 + \frac{\langle \mathbf{A}_1 \mathbf{A}_2^* \rangle}{(\langle |\mathbf{A}_1|^2 \rangle \langle |\mathbf{A}_2|^2 \rangle)^{1/2}}. \quad (10)$$

Substituting Eqs. (2) and (3) into Eq. (10) and evaluating the integrals yield

$$\boldsymbol{\mu}_I(\Delta x, \Delta y, z, \tau) - 1 = \exp\left(-\frac{v^2\tau^2}{\omega^2}\right) \times \exp\left\{-\frac{\left[\Delta x - \left(1+\frac{z}{\rho}\right)v\tau\right]^2 + \Delta y^2}{r_s^2}\right\}, \quad (11)$$

in the vicinity of the optical axis. In Eq. (11), r_s signifies the speckle pattern's linear correlation length over the observation plane, which may be interpreted as the average radius of an individual speckle lobe, given

$$r_s = \frac{\lambda z}{\pi \omega}. \quad (12)$$

Equation (11) is almost identical to the expression given by Yoshimura [6] and Takai *et al.* [7] for a transmission coordinate system. While not immediately apparent, there is a major difference for PDV's single degree of freedom geometry, in that the values of ρ, ω, and r_s are coupled to the axial displacement z according to Eqs. (4), (5), and (12). As we will see in

Table 1. Beam Shape Parameters for the Focusing (1) and Collimating (2) Optical Probes Used in PDV Experiments

Probe	Focal Length	Beam Waist
	(z_f) (mm)	(ω_0) (μm)
1	20	23
2	100	50

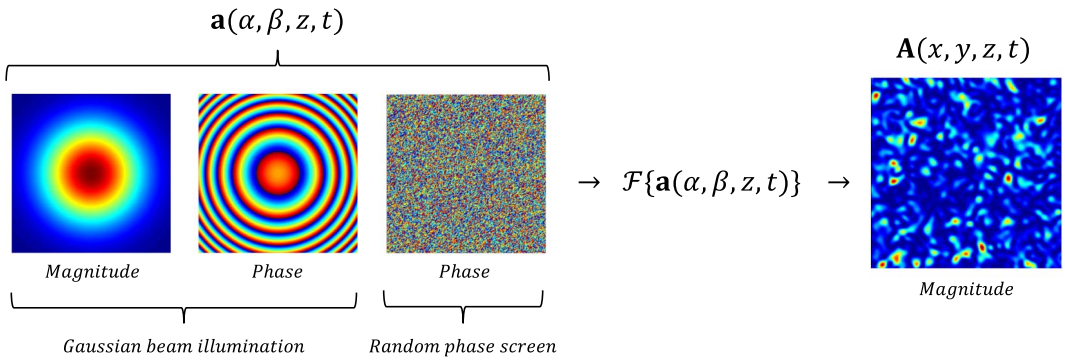

Fig. 2. To numerically simulate a speckle pattern, we first generate a discretized Gaussian illumination function and random-phase screen, which are superimposed to yield the scattered field $\mathbf{a}(\alpha,\beta,z,t)$. The scattered field is then propagated out to the observation plane via a Fourier-transformation.

the following analysis, this coupling results in vastly different speckle dynamics.

Simulating speckle dynamics is relatively straight forward. For each iteration or time step, the discretized random-phase screen $\phi(\alpha,\beta)$ is shifted by one discrete step in the positive α direction with respect to the illumination, and a new speckle pattern is produced. As the iteration number increases, so does the cumulative displacement of the random-phase screen from its original position. Figure 3 shows how the correlation function is numerically generated by convolving the speckle pattern produced for $\tau = 0$, with subsequent speckle patterns produced when $\tau > 0$. In addition, Fig. 3 shows how correlation and translation measurements are extracted from the simulation by finding the coordinates and value of the correlation function's global maximum.

Intuitively, it makes sense that, as the scattering surface is gradually displaced from its original position at $v\tau = 0$, the resulting speckle pattern will gradually diverge from its original spatial structure, becoming less correlated. The physical basis for this decorrelation is the substitution of new surface scatterers into the illuminated beam spot in place of the original population. It follows that the degree to which a speckle pattern remains correlated is in direct proportion to the ratio of original surface area that remains within the illuminated beam spot. Evaluating the first term of Eq. (11), we see that the speckle pattern loses coherence (that is to say, the correlation drops to e^{-1}) once the scattering surface displacement satisfies

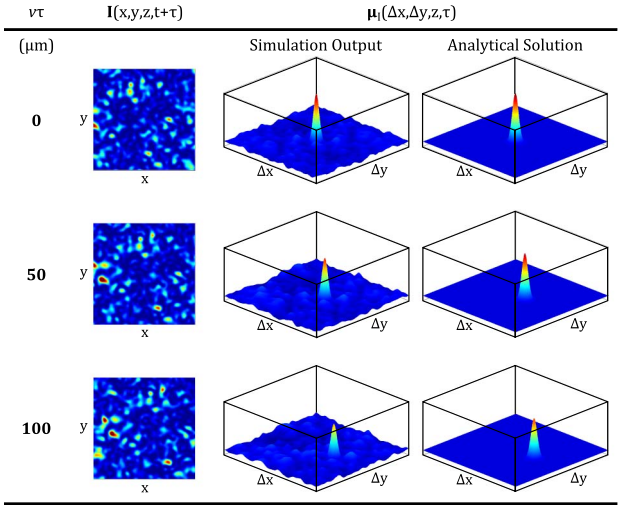

Fig. 3. Simulated speckle patterns and correlation functions generated for a surface translating in the positive α direction, illuminated by Probe 1 with $z = 30$ mm. It is evident by looking at the sequential snapshots of the speckle pattern that its bulk motion is in the positive x direction (toward the right side of the page) and this is reflected by the location of the correlation function's peak value as it is displaced in the positive Δx-direction. As the scattering surface moves further from its original position at $v\tau = 0$, the speckle pattern becomes less correlated, reducing the correlation function's peak value.

$$v\tau_t = \omega, \tag{13}$$

at which point the ratio of original surface area remaining within the illuminated beam spot is also e^{-1}. We refer to $v\tau_t$ as the *surface translation length*. This provides some insight into why a greater degree of boiling is observed when the scattering surface is located at the laser beam focal point: the illuminated beam spot is at its smallest size. Theoretical and simulation results for the surface translation length are shown in Fig. 4. Some of the simulation results show surface translation lengths that are smaller than the analytical model predicts, likely due to quantization errors in the simulation.

Values of $(\Delta x, \Delta y)$ maximizing the second term of Eq. (11) correspond to the translation vector of the speckle pattern as a function of scattering surface displacement. Setting $v\tau = \omega$, we find the total translation vector of the speckle pattern at the instant it loses coherence is given

$$\Delta x_t = \left(1 + \frac{z}{\rho}\right)\omega \quad \Delta y_t = 0, \tag{14}$$

which confirms that the speckle pattern's translation is along the same linear axis as the scattering surface. We define the magnitude of vector $(\Delta x_t, \Delta y_t)$ as the *speckle translation length*. Simulation results are shown in Fig. 5. Equations (13) and (14) show that the speckle and surface translation lengths are not equivalent. Recognizing that these displacements take place over the same amount of time, we solve for the speckle pattern translation rate V_s relative to surface speed v as the quotient of the displacements, yielding

$$\frac{V_s}{v} = \left(1 + \frac{z}{\rho}\right). \tag{15}$$

As shown in Fig. 6, the speckle pattern translation rate widely varies from that of the scattering surface,

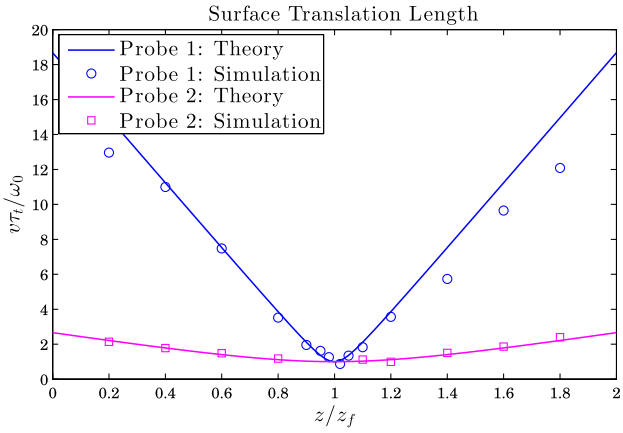

Fig. 4. Total translation length $v\tau_t$ of the surface at the instant in which the correlation between $\mathbf{I}_1$ and $\mathbf{I}_2$ drops to e^{-1}, normalized against the beam waist ω_0. We may think of the surface translation length as the length-scale associated with boiling.

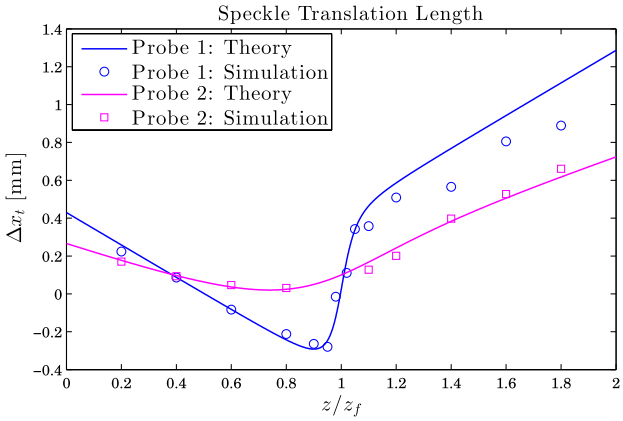

Fig. 5. Total translation length of speckle along the x-axis of the observation plane at the instant in which the correlation between $\mathbf{I}_1$ and $\mathbf{I}_2$ drops to e^{-1}. Both analytical predictions and simulation results found that $\Delta y_t = 0$ for all values of z/z_f.

depending upon the location of the surface along the laser beam. Naturally, in the limit of $z = 0$, complex field $\mathbf{A}$ is incident on the surface where it translates in parallel, yielding $V_s/v = 1$. As the scattering surface approaches the focal point of Probe 1, there is a regime where speckle pattern translation is in the opposite direction to that of the scattering surface. In general, we find that scattering surface translation is magnified in the speckle pattern for optical probes with greater relative convergence.

By now, it should be clear that speckle pattern motion does not simply mirror scattering surface motion. Instead, there are strong parametric dependencies on the laser beam used for illumination as well as the offset distance between the scattering surface and observation plane. Although speckle is a random process, speckle dynamics are predictable in the statistical sense and have been fully characterized for the PDV coordinate system and optical configuration. Boiling is a consequence of surface translation and has an associated length-scale determined by the radius of the illuminated beam spot ω, and

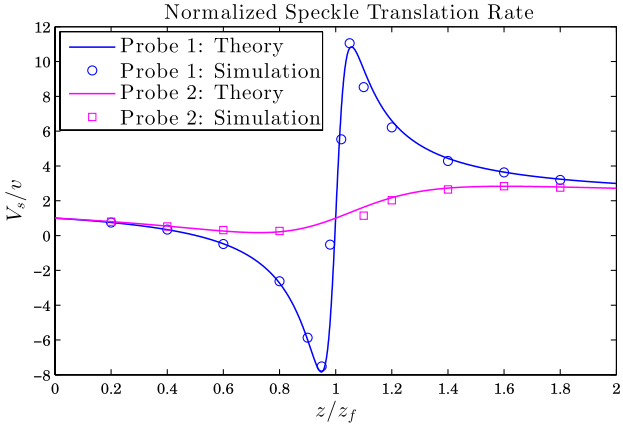

Fig. 6. Speckle translation rate V_s normalized against the surface translation rate v. Speckle translation is greatly magnified when the scattering surface is located near the focal point of Probe 1, and actually moves in the opposite direction for $z/z_f \in (0.5, 1)$.

results in speckle pattern decorrelation. Speckle translation rate with respect to the scattering surface is determined by the location of the surface along the beam, as well as the relative convergence of the beam.

C. Speckle in the PDV Signal

In the previous section, we examined the normalized correlation function of the diffracted electric field, which relates bulk properties of speckle motion to that of the scattering surface. PDV does not provide the full-field observation capability required to observe bulk speckle motion. Instead, intensity measurements are taken at a small, finite-sized point in the diffracted electric field and we are left to infer surface motion from the speckle intensity fluctuations that take place within this locale. Rather than observing a detailed video of the speckle pattern changing in time, the PDV probe is akin to a single enlarged pixel.

Fortunately, for any given illumination geometry and set of optical parameters, there exists a linear relationship between the average time scale of local intensity fluctuations at the PDV probe and the rate of scattering surface translation. If we adopt the assumption of pure speckle translation, then this relationship is relatively straight forward: the average time scale of speckle intensity fluctuations corresponds to the average amount of time required for a speckle to pass over our probe. In application, the time scale of local intensity fluctuations is also related to the rate at which boiling modifies the spatial structure of the speckle pattern.

To evaluate analytically the time scale of local intensity fluctuations that are produced and spatially integrated in the observation plane by our circular PDV probe, we must consider the normalized correlation function of spatially integrated speckle, expressed

$$\boldsymbol{\mu}_W(z,\tau) = \frac{\langle \boldsymbol{W}(z,t)\boldsymbol{W}(z,t+\tau)\rangle}{\langle \boldsymbol{W}(z,t)^2\rangle}, \tag{16}$$

where $\mathbf{W}(z,t)$ is the instantaneous integrated intensity defined in Eq. (7). While an exact solution for this expression has not been found due to mathematical complexity, Iwai *et al.* show that the circular aperture function we introduce in Eq. (8) is well approximated by a *soft Gaussian aperture* [18]. Adopting the soft Gaussian aperture approximation and evaluating Eq. (16), the normalized correlation function of spatially integrated speckle takes the form

$$\boldsymbol{\mu}_W(z,\tau) = \exp\left(-\frac{v^2\tau^2}{\omega^2}\right) \times \exp\left[-v^2\tau^2\frac{(1+z/\rho)^2}{R^2+r_s^2}\right], \tag{17}$$

where the average time scale of speckle intensity fluctuations, measured by a Gaussian aperture of radius R, is expressed

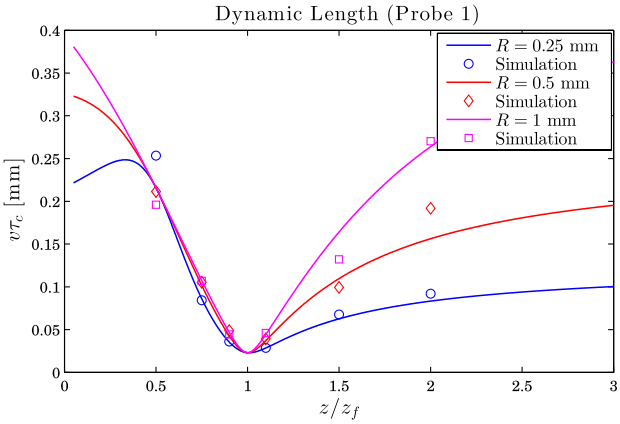

Fig. 7. Solid curves correspond to theoretical dynamic lengths for spatially integrated speckle using a focusing probe (Probe 1) and Gaussian soft apertures of different radii. Simulated data points correspond to identical optical conditions and hard circular apertures.

$$\tau_c = \frac{1}{v\left[\frac{1}{\omega^2} + \frac{(1+z/\rho)^2}{R^2+r_s^2}\right]^{1/2}}. \tag{18}$$

If we evaluate $v\tau_c$, referred to as the *dynamic length*, then we end up with the characteristic length-scale of scattering surface displacement required for the aperture to see new, uncorrelated speckles. The dynamic length is valuable to consider because it is invariant to the rate of surface translation; instead, exposing the underlying parametric dependencies of speckle intensity fluctuations in the PDV signal. In Fig. 7, there is a clear drop in dynamic length when the scattering surface is located at the laser beam focal point, which is in agreement with recent experimental observations [14].

For an aperture of infinite surface area, $R \to \infty$ and the aperture function $\boldsymbol{D}(x,y)$ goes to unity. In this case, we essentially cross-correlate the full spatially-integrated diffracted field; as a result, all speckle dynamics are captured by the aperture, and the dynamic length $v\tau_c$ reaches its maximum possible value of ω. For smaller apertures, it becomes possible for the speckle translation length $|(\Delta x_t, \Delta y_t)|$ to exceed the length-scale of the aperture, effectively resulting in a pure translation measurement. When this is true, the dynamic length becomes sensitive to the length-scale of both the aperture and individual speckles. In Fig. 7, we see the dynamic length decrease with the size of the aperture except for at points $z/z_f = \{0.5, 1\}$, where it remains constant for all apertures shown. At these points, the speckle translation rate V_s goes to zero for nonzero surface speed v (see Probe 1 in Fig. 6). Under this pure boiling condition, an aperture of any size will observe the speckle pattern descend into disorder at the same rate.

Simulated PDV signals were produced by numerically integrating the circular aperture function in Eq. (8) over the diffracted intensity field in the observation plane for a series of speckle patterns, yielding an instantaneous integrated intensity time-series. Ten thousand speckle patterns were produced and spatially integrated for each tested set of parameters. Typically, the radius of a circular PDV probe aperture is around 1 mm, so simulations were carried out for apertures with radii of 0.25, 0.5, and 1 mm. Figure 8 provides a visualization of the process we used to simulate PDV time-series and generate the correlation function of spatially integrated speckle via numerical autocorrelation.

Simulation results closely approximate their predicted values with a few exceptions; the exceptions are likely due to our use of a 10,000 data point time-series in the numerical autocorrelation. In PDV applications, it is common to use in the range of 25,000–50,000 data points to generate a more statistically robust autocorrelation curve, but this was impractical from the simulation standpoint, where computational resources were limited.

4. Conclusions

The characteristic time scale of speckle intensity fluctuations in the PDV signal is directly related to speckle dynamics, which, in turn, are related to lateral surface speed. Various parametric dependencies exist between the shape and geometry of the illuminating laser beam and the resulting speckle dynamics; we characterized these dependencies analytically via the space–time correlation function of the diffracted electric field and substantiated them through

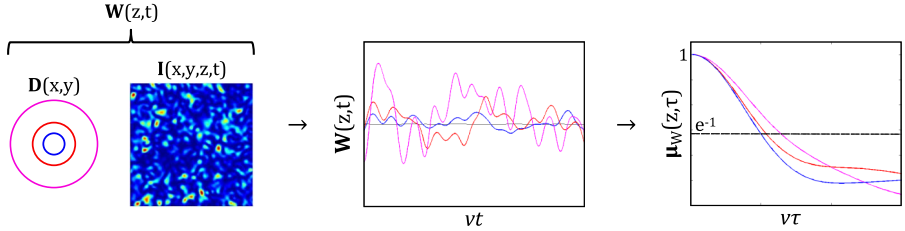

Fig. 8. PDV signal $\boldsymbol{W}(z,t)$ is simulated by numerically integrating our aperture function $\boldsymbol{D}(x,y)$ over the intensity field in the observation plane (three aperture functions are shown above). After 10,000 iterations, we build up a time-series (center), where the vertical axis represents instantaneous integrated intensity and the horizontal axis corresponds to cumulative displacement of the scattering surface. Numerical autocorrelation is performed on the signal yielding $\boldsymbol{\mu}_W(z,\tau)$ (right) and the dynamic length is given by the value of $v\tau$, where the correlation function drops to e^{-1}. For the particular optical arrangement used in this example, dynamic length increases with the radius of our circular aperture function.

numerical simulation. By evaluating the normalized correlation function of spatially integrated speckle, we related the size of a detecting aperture to the characteristic time-scale of speckle intensity fluctuations in the PDV signal. Analytical and simulation results show close agreement and qualitatively agree with recent experimental findings.

This work holds immediate relevance to PDV and other single-beam optical velocimetry applications where speckle is observed, potentially providing a basis for simultaneously measuring a surface's axial velocity and lateral speed with a single probe. Future work must examine how dynamic speckle manifests in the PDV signal when an axial velocity component is included in the surface velocity vector. Such a solution could be directly applied to PDV data, allowing experimentalists to extract axial velocity via conventional Fourier-analysis and lateral speed via analysis of speckle intensity fluctuations.

References

1. B. Jensen, D. Holtkamp, P. Rigg, and D. Dolan, "Accuracy limits and window corrections for photon Doppler velocimetry," J. Appl. Phys. **101**, 013523 (2007).
2. D. Dolan, "Accuracy and precision in photonic Doppler velocimetry," Rev. Sci. Instrum. **81**, 053905 (2010).
3. L. G. Shirley, E. D. Ariel, G. R. Hallerman, H. C. Payson, and J. R. Vivilecchia, "Advanced techniques for target discrimination using laser speckle," L. Lab. J. **5**, 367–440 (1992).
4. J. W. Goodman, "Statistical properties of laser speckle patterns," in *Laser Speckle and Related Phenomena* (Springer, 1975), pp. 9–75.
5. J. Dainty, "An introduction to Gaussian speckle," Proc. SPIE **243**, 2–8 (1980).
6. T. Yoshimura, "Statistical properties of dynamic speckles," J. Opt. Soc. Am. A **3**, 1032–1054 (1986).
7. N. Takai, T. Iwai, and T. Asakura, "Correlation distance of dynamic speckles," Appl. Opt. **22**, 170–177 (1983).
8. I. Yamaguchi and S.-I. Komatsu, "Theory and applications of dynamic laser speckles due to in-plane object motion," J. Mod. Opt. **24**, 705–724 (1977).
9. T. Asakura and N. Takai, "Dynamic laser speckles and their application to velocity measurements of the diffuse object," Appl. Phys. **25**, 179–194 (1981).
10. N. Takai, T. Iwai, T. Ushizaka, and T. Asakura, "Velocity measurement of the diffuse object based on time-differentiated speckle intensity fluctuations," Opt. Commun. **30**, 287–292 (1979).
11. J. Ohtsubo, "Velocity measurement using the time–space cross-correlation of speckle patterns," Opt. Commun. **34**, 147–152 (1980).
12. T. Iwai, N. Takai, and T. Asakura, "Dynamic statistical properties of laser speckle produced by a moving diffuse object under illumination of a Gaussian beam," J. Opt. Soc. Am. A **72**, 460–467 (1982).
13. E. A. Moro and M. E. Briggs, "Note: simultaneous measurement of transverse speed and axial velocity from a single optical beam," Rev. Sci. Instrum. **84**, 016110 (2013).
14. E. A. Moro, M. E. Briggs, and L. M. Hull, "Defining parametric dependencies for the correct interpretation of speckle dynamics in photon Doppler velocimetry," Appl. Opt. **52**, 8661–8669 (2013).
15. W. J. Warren, L. Ott, E. Elmore, E. A. Moro, and M. E. Briggs, "Laser speckle in dynamic sensing applications," in *Special Topics in Structural Dynamics* (Springer, 2014), Vol. **6**.
16. J. W. Goodman, *Introduction to Fourier Optics* (Roberts, 2005).
17. J. W. Goodman, *Speckle Phenomena in Optics: Theory and Applications* (Roberts, 2007).
18. T. Iwai, N. Takai, and T. Asakura, "The autocorrelation function of the speckle intensity fluctuation integrated spatially by a detecting aperture of finite size," J. Mod. Opt. **28**, 1425–1437 (1981).